

ORIGINAL ARTICLE

Cell effects on the formation of collagen triple helix fibers inside collagen gels or on cell surfaces

Chun-Yen Liu, Michiya Matsusaki and Mitsuru Akashi

Collagen molecules are widely used in the field of tissue engineering, especially as cell culture hydrogels. However, the cellular effects on collagen fiber formation inside collagen gels have not been reported. Here, we evaluated the effect of cells on collagen triple helix fiber formation at a molecular level in collagen hydrogels or on cell surfaces. Swelling ratios of collagen gels decreased with increasing cell numbers, most likely because of interactions between cell surface integrin molecules and collagen fibers. Circular dichroism and ultraviolet–visible spectroscopic analyses revealed aggregations of cells and collagen molecules because of their strong interaction. X-ray diffraction analyses suggested that cells did not affect the weak molecular orientation of collagen fibers inside collagen gels because the collagen gels usually do not have as dense molecular packing as natural collagen fibers in tendons. Scanning electron microscopy showed aggregations of submicrometer-sized spherical collagen structures mainly around cells inside collagen gels. The results suggest that interactions between cell surfaces and collagen molecules induce the formation of spherical constructs rather than microfibril formation, which in turn indicates that interactions between cells and collagen molecules induce the adsorption of collagen molecules onto cell surfaces and lead to the formation of spherical constructs in hydrogels.

Polymer Journal (2015) 47, 391–399; doi:10.1038/pj.2015.2; published online 18 February 2015

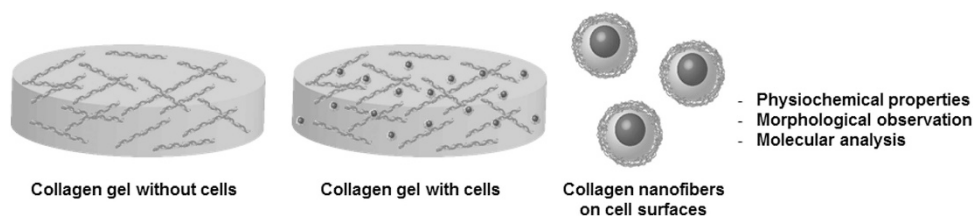
INTRODUCTION

In human bodies, tissues and organs are composed of cells with various types of extracellular matrices (ECMs). ECMs provide physical support to tissues by occupying the intercellular space, acting not only as benign native scaffolding for arranging cells within connective tissues but also as a dynamic, mobile and flexible substance in regulating cellular behaviors and tissue functions. Among these ECMs, collagen is the most abundant structural protein found in the human body and is the major and most abundant component of animal connective tissues, such as cartilage, cornea, bones, blood vessels or muscle tissues.^{1,2} There are many approaches to replace or improve the biofunction of tissues or organs involving three-dimensional (3D) scaffolds. Substances such as natural polymeric materials, synthetic polymers and biodegradable polymers are usually chosen as target compounds. Among these materials, collagen is widely used in the application of tissue engineering owing to its high biocompatibility with many tissues and its biodegradability. Furthermore, collagen determines cell adhesion, cell phenotype and has a role in regulating cells and tissues.

There are at least 16 types of collagen, but 80–90% of the collagen in the body consists of types I, II and III. Among these collagen types, type I collagen is the most widely used material in biomedical or tissue engineering fields and is easily denatured by environmental temperatures and pH.^{3–5} Collagen molecules have rod-like triple-helical structures consisting of three polypeptide chains. The most common motif in the amino-acid sequence of collagen is glycine-proline-X or

glycine-X-hydroxyproline, where X indicates any amino acid other than glycine, proline or hydroxyproline. Five triple-helical molecules further assemble to form a microfibril, and microfibrils assemble to form collagen fibrils with 10–300 nm diameters. The diameters of fibrils change slightly along their length, with a highly reproducible D-band repeat of ~67 nm. *In vivo*, collagen fibrils organize in one direction to form collagen fibers of 0.5–3 μm in tendons or ligaments (Supplementary Figure S1). The orientation of these collagen molecules is known to be a significant factor in the mechanical strength of natural tissues.

Cellular function in two-dimensional (2D) and 3D cultures is different because of the limited interactions between cells and their microenvironments in 2D cultures. In 3D cell cultures, enhanced cellular interactions are achieved with cells and ECMs.^{6,7} Various 3D cell culture systems, such as matrix-embedded cultures,^{8–13} cellular multilayers^{14,15} and *ex vivo* cultures,^{16,17} have been developed to mimic *in vitro* microenvironments. These methods are widely used in both micro- and macrosystems in various studies because of their simplicity and versatility. However, the cellular effect on collagen fiber formation inside collagen gels has not been reported. The α2β1-integrin receptors,^{18,19} which can interact with collagen fibers, are embedded in cell surface membranes,²⁰ with an association constant of $6.7 \times 10^4 \text{ M}^{-1}$.¹ These data suggest that the embedded cells inside collagen hydrogels should interact with collagen triple helix fibers and may induce some effects on collagen fiber structures. Collagen triple helix fibers are important for both maintaining the mechanical



Scheme 1 Schematic illustration of collagen gels with or without cells and collagen nanofibers on the cell surfaces. A full color version of this figure is available at *Polymer Journal* online.

Table 1 Sample conditions in this study

	Concentration (wt%)	Cell number (cells)
<i>Collagen gels</i>		
Without cells	0.03	—
	0.1	—
	0.2	—
	0.3	—
With cells	0.03	1×10^4
		1×10^5
		1×10^6
	0.1	1×10^4
		1×10^5
		1×10^6
	0.2	1×10^4
		1×10^5
		1×10^6
		1×10^4
		1×10^5
		1×10^6
0.3	1×10^4	
	1×10^5	
	1×10^6	
<i>Collagen nanofibers on cell surfaces</i>	0.03	1×10^6

strength of matrices and interactions with growth factors or cytokines produced in cells. Moreover, they provide sufficient ECM microenvironments to cells to provide signals for growth, differentiation, migration and apoptosis.²¹

We recently reported a unique coating technology of type I collagen nanofibers on cell surfaces.²² Based on specific interactions between collagen molecules and integrin receptors in cell membranes,^{23,24} collagen fibers are formed controllably on cell surfaces in a way that coincides with the ‘ball of wool’ model. Using this technique, we fabricated collagen nanofiber layers of varying thickness on cell surfaces and constructed stable, thick, 3D tissues with different cell densities.

In this study, we examined cell effects on collagen triple helix fiber formation at the molecular level inside collagen gels. As shown in Scheme 1, cell effects on collagen fiber formation on cell surfaces using our collagen nanofiber coating were compared with the effects on collagen gels. Through various characterizations, we found that strong adsorption of collagen molecules onto cell surfaces led to the formation of collagen molecules around the cell. However, nanometer-sized collagen fiber network formation on cell surfaces was observed after applying the coating method. Based on the results of this study, we describe for the first time cell effects at the molecular level on collagen fiber formation in hydrogels and on cell surfaces.

MATERIALS AND METHODS

Materials

Human dermal fibroblast cells were purchased from Cambrex (East Rutherford, NJ, USA). Type I collagen solution (from bovine corium, 0.3 wt

%, 5 mM acetic acid) was purchased from Nippi Company (Tokyo, Japan). Dulbecco’s modified Eagle’s medium (DMEM), 10% formalin solution (4% formaldehyde in water containing methanol), trypsin and 1 M NaOH were from Wako Pure Chemical Industries (Osaka, Japan). Fetal bovine serum was purchased from Biowest (Miami, FL, USA). The antibiotics were purchased from Nacalai Tesque (Kyoto, Japan). The culture medium, Petri dish and centrifugation tube were purchased from AGC Techno Glass (Shizuoka, Japan). The plastic tube was purchased from Sumitomo Bakelite (Tokyo, Japan). All reagents were used without further purification.

Cell culture

Normal human dermal fibroblast cells at passages 5–9 were cultured in DMEM with 10% fetal bovine serum and 1% antibiotics at 37 °C in a humidified 5% CO₂ incubator. During each passage, normal human dermal fibroblast cells were treated with 3 ml of 0.1% trypsin for 20 min to detach them from the culture media. Detached cells were then collected in a 15 ml plastic tube containing 4 ml of DMEM and centrifuged at 1000 r.p.m. for 5 min. The supernatants of the centrifuged solutions were removed, and fresh DMEM was added into the plastic tube for calculating the cell numbers or to be used in further experiments.

Preparation of collagen gels with and without cells

In this study, collagen gels with and without living cells were prepared and characterized. As shown in Table 1, four different concentrations of collagen solutions were prepared by diluting with 5 mM acetic acid. Each prepared collagen solution contained various cell numbers: no living, 1×10^4 , 1×10^5 and 1×10^6 cells.

After preparing collagen solutions with different numbers of cells, the prepared solutions were poured into a 35-mm Petri dish and moved into an incubator (37 °C with humidified 5% CO₂) for ~24 h to wait for the formation of collagen gels. The collagen gels were then freeze-dried for 3 days. The swelling ratios of these different gels were calculated by measuring variations in gel weight. Additionally, dried gels were used for circular dichroism (CD), Fourier transform infrared (FTIR), X-ray diffraction (XRD) and scanning electronic microscope (SEM) analyses.

Preparation of collagen nanofibers on single-cell surfaces

In this part of the experiment, collagen nanofibers were coated onto cell surfaces by their strong interactions with $\alpha 2\beta 1$ -integrin receptors in the cell surfaces with an association constant of $6.7 \times 10^4 \text{ M}^{-1}$. From previous reported results, certain parameters such as collagen concentration, rotation speed, temperature and cell number may affect the coating results. After a series of optimization experiments, we set 0.03 wt% collagen with 1×10^6 cells under 37 °C at 50 r.p.m. for at least 20 min as the standard coating conditions.²²

As in a previously reported method, 120 μl of 5x DMEM, 60 μl of fetal bovine serum, 20 μl of distilled H₂O and 8 μl of 1 M NaOH were mixed together. Next, 600 μl of DMEM with normal human dermal fibroblast cells was added into the prepared solutions. After mixing, 400 μl of 0.03 wt% collagen solution was gently added into the solution via a pipette. The prepared solutions were moved to a 37 °C oven for ~20 min. After the coating step, the solutions were poured into 15 ml plastic tubes and washed two times with phosphate-buffered saline to remove unreacted molecules. The washed solutions were then centrifuged to collect collagen-coated cells. Collected samples were characterized by CD, FTIR, XRD and SEM and compared with results from collagen gels with and without cells.

CD spectral analyses

Collagen molecules used for the gel formation and coated onto cell surfaces were purchased from Nippi Company. The purchased collagen was already dissolved in 5 mM acetic acid (0.3 wt%) and stored at 4 °C. The collagen samples were adjusted to 0.003 wt% using 5 mM acetic acid before CD analysis. Samples of 0.003 wt% collagen solutions with and without the addition of cells treated under various temperatures (25 and 37 °C) and pH conditions (pH 4 and 7) were prepared and examined in this study. Sample solutions were scanned at a wavelength range from 200 to 260 nm, and the molar ellipticity [θ] was recorded using a CD apparatus (J-725; Jasco, Tokyo, Japan). In addition, 0.003 wt% collagen solution with and without 1×10^4 cells under different temperatures and pH values were prepared for 24 h observation to examine variations in collagen structures. Collagen-coated cells under various temperature and pH conditions were also prepared for CD spectral analysis.

FTIR spectra analyses

Collagen gels with and without cells, cells and collagen-coated cells were characterized by FTIR spectroscopy recorded using a Perkin-Elmer Spectrum One instrument (Perkin-Elmer Inc., Waltham, MA, USA). All spectra were treated using baseline correction.

XRD spectra analyses

All samples prepared in this study (Table 1) were fixed onto a cover glass. The XRD patterns were recorded on a RIGAKU RINT 2000 instrument (Rigaku, Tokyo, Japan) with a $\text{CuK}\alpha$ ($\lambda = 0.154$ nm) source at room temperature, operated at 40 kV and 200 mA. Samples were examined at $2\theta/\theta$ equal to $5\text{--}50^\circ$ with a measuring time of 1 min per 2° .

SEM observations

The morphological properties of collagen gels with and without cells were observed by SEM (JSM-6700F; JEOL, Tokyo, Japan) at 5 kV, whereas low-voltage SEM instrument (Miniscope TM3030; Hitachi, Tokyo, Japan) at 5 kV was applied to observe cells and collagen-coated cells. Collagen gels with and without cells were freeze-dried directly after a 24 h incubation in a 37 °C incubator. Dried samples were moved onto a carbon tape and coated with osmic acid for SEM observations. In the case of cells and collagen-coated cells, all samples were fixed by 10% formalin for 15–20 min and washed two times with phosphate-buffered saline to remove formalin from the samples. Before staining with TI blue, the cell samples were loaded onto porous membranes (ISOPORE membrane filter, 3 μm diameter; Millipore, Darmstadt, Germany) and washed two times with distilled water. Then, 200 μl of ammonium solution was used to prepare TI (particulate titanium) blue staining solution with a staining kit (Nisshin EM, Tokyo, Japan). The prepared TI blue solution was dropped onto washed samples and stained for 20–30 min. After staining, the

samples were washed two times with distilled water to remove excess TI blue solution. Stained samples were fixed onto a carbon tape and then observed using SEM.

RESULTS AND DISCUSSION

Cell effects on the formation of collagen gels

In this experiment, we used the usual collagen concentrations for 3D cell cultures, 0.3 wt% in 5 mM acetic acid conditions, based on the formulation from Nippi company.²⁵ Based on our previous publication,²² we applied 0.03 wt% collagen to fabricate collagen nanofiber matrices on cell surfaces. Hence, a concentration range from 0.3 to 0.03 wt% was chosen as a target in the following collagen gel experiments. Collagen molecules easily formed into gel states in 37 °C neutralized solution, and all prepared collagen gel samples formed into gel states after 24 h incubation.

As shown in Figure 1, we obtained almost the same swelling ratio for all collagen concentrations, even though the size of the pure collagen gels was dependent on the collagen concentration. Higher collagen concentration resulted in thicker collagen gels after 24 h of incubation, whereas thinner collagen gels were formed with lower collagen concentrations (Supplementary Figure S2). However, once cells were added to the collagen gels at 0.1, 0.2 and 0.3 wt%, the swelling ratio decreased with increasing cell number because additional crosslinking forces inside the collagen gels. As known previously, interactions between integrin $\alpha 2\beta 1$ receptors and collagen molecules are very strong ($6.7 \times 10^4 \text{ M}^{-1}$)²⁶ and may therefore be considered to act as crosslinkers in this collagen gel system, leading to smaller swelling ratios with an increase in cell number. In the case of the highest cell number (1×10^6 cells), the collagen gels shrank with higher collagen concentrations. This finding may be because cells adhered to and spread on collagen fiber matrices, leading to strong interactions between collagen molecules and cell surfaces inside collagen gels, resulting in the detachment and shrinking of collagen gels from the substrates.²⁷

In the case of 0.03 wt% collagen gels, we found that there was no cell effect even with the addition of cells. In the 0.03 wt% collagen gel system, the crosslinking point might be lower than with the other three collagen concentrations owing to the low collagen concentration. Interactions between collagen molecules and the cell surface did not occur, and no extra crosslinking forces were formed inside the collagen gels. This may be the reason why the presence of cells had no effect when using the 0.03 wt% collagen gels. To understand the effect of cells on collagen triple-helical structures, CD, IR and XRD spectral analyses were performed.

Effects of cells on the amide bands of collagen molecules

Collagen is an optically active protein with two prominent parts: a negative minimum absorption band at ~ 210 nm, which indicates the characteristic random coil of collagen, and a positive maximum absorption band at 223 nm, characteristic of collagen triple helices. To measure the CD spectra of collagen molecules, 100-fold diluted collagen solutions (0.003 wt%) were used due to instrument limitations. In this experiment, 5 mM acetic acid buffer was used as the solvent, and we confirmed there was no effect on cell viability during a minimum incubation of 2 h. CD spectra were measured both at 25 and 37 °C because some researchers have reported instability in collagen triple-helical structures at 37 °C.^{3,4} Harris *et al.*⁵ reported collagen fiber formation and subsequent gelation occurring under neutral pH conditions. Accordingly, we measured CD spectra under both acidic and neutral pH conditions.

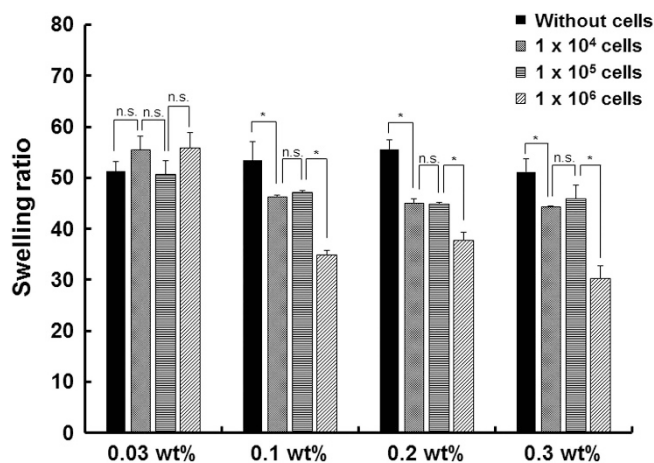


Figure 1 Swelling ratio of collagen gels with and without the addition of normal human dermal fibroblasts (NHDFs) under different collagen concentrations ($n=3$; $*P<0.05$; NS, no significant difference).

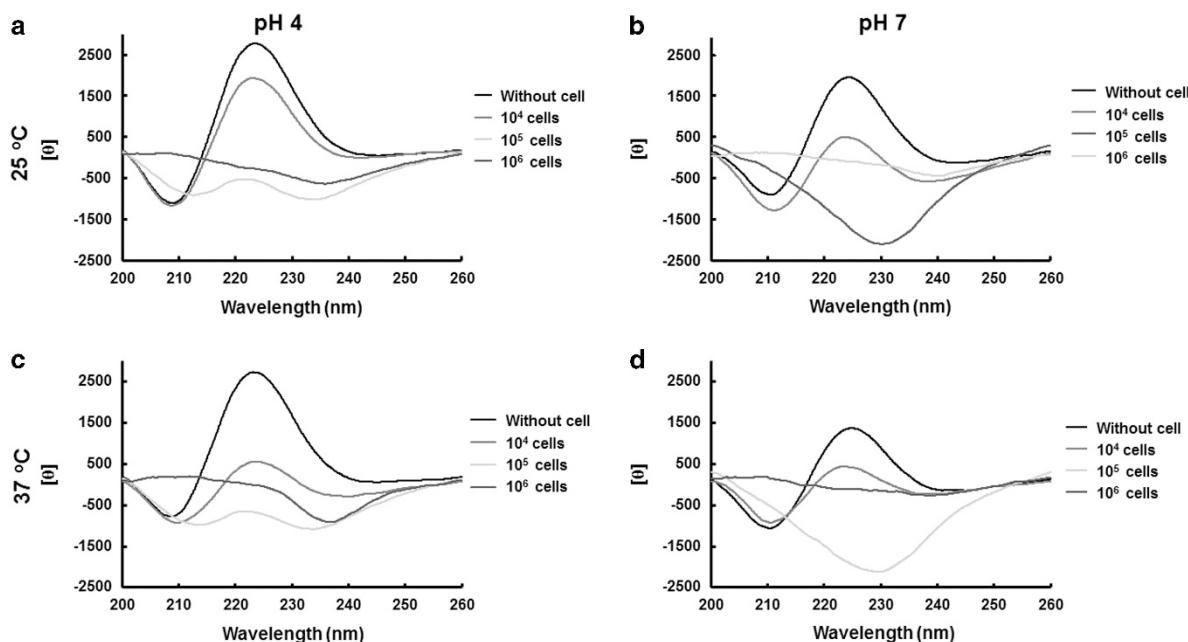


Figure 2 Circular dichroism (CD) spectra of 0.003 wt% collagen solution with or without cells in pH 4 or 7 solutions at (a, b) 25 °C or (c, d) 37 °C after a 2-h incubation. A full color version of this figure is available at *Polymer Journal* online.

Normally, collagen triple-helical structures have strong positive peaks at 223 nm. As shown in Figure 2a, when 1×10^4 cells were added to 0.003 wt% collagen solutions at pH 4, the triple helix peak decreased from $[\theta_{223}] = 2700$ to 1900. When the cell number increased to over 1×10^5 cells, the triple helix peak disappeared. Under neutral pH conditions, the collagen triple helix peak was slightly lower than under acidic conditions ($[\theta_{223}] = 1900$). When 1×10^4 cells were added, triple helix peaks significantly decreased to $[\theta_{223}] = 500$ and disappeared entirely when 1×10^5 cells were added (Figure 2b). The reason for the decrease in the peaks might be aggregation of collagen and cells or the dissociation of the triple-helical structures. To evaluate the formation of collagen aggregates, transmittance (%T) of the collagen solutions was measured at 223 nm for 1 h (Supplementary Figure S3). In the cases of both pH 4 and 7, a 0.003 wt% collagen solution itself was used as the background (100 %T). When 1×10^4 cells were added, %T decreased slightly to 70, and 90% at pH 4 and pH 7, respectively, suggesting that there was no formation of aggregates inside the collagen solutions. However, with over 1×10^5 cells, 50 %T was measured during a 1 h incubation. We clearly identified some aggregation inside the cuvettes upon visual inspection, and aggregation was observed immediately after mixing with the cell solution. These results suggest that the formation of aggregates with collagen molecules lead to decreases in triple helix peaks. Triple helical structures should remain after mixing with cells. These results also showed that cell surfaces act as crosslinkers for collagen fibers (Figure 1).

When the temperature was increased to body temperature, 37 °C, triple helix peaks at pH 7 decreased slightly, but there was no difference at pH 4. Triple helix peaks for the pH 4 solution significantly decreased to $[\theta_{223}] = 500$ even with 1×10^4 cells (Figure 2c). Temperature may induce interactions between collagen molecules and cell surfaces, and triple helix peaks decreased to $[\theta_{223}] = 300$, which was the lowest value of $[\theta]$ with 1×10^4 cells. From these results, we note that body temperature and neutral pH stimulated strong interactions between collagen molecules and cell

surfaces. Additionally, as shown in Supplementary Figure S3, transmittance (%T) of collagen solutions with 1×10^5 and 1×10^6 cells at both pH 4 and 7 had ~ 40 %T and 20 %T, indicating that aggregation occurred inside the collagen solutions.

To understand the time dependency between collagen molecules and cell surfaces, we evaluated time-dependent CD spectral changes under various conditions. As shown in Figure 3a, the sample without cells, at pH 4 and 25 °C showed little change after 24 h incubation ($[\theta_{223}] = 3000$ to $[\theta_{223}] = 2800$). When 1×10^4 cells were added to the collagen solutions, the triple helix peaks immediately decreased to $[\theta_{223}] = 1800$ (1 min incubation) and remained constant after 24 h incubation. In the case of the pH 7 solution at 25 °C (Figure 3b), triple helix peaks decreased significantly to $[\theta_{223}] = 600$ after 1 min of incubation and then decreased continuously during 24 h of incubation. These results suggest that interactions between collagen molecules and cell surfaces at neutral pH occur continuously over a 24-h incubation period, although there was no continuous decrease of the triple helix peak under acidic conditions.

When the temperature of the pH 4 solutions increased to 37 °C, a significant decrease of triple-helical peaks was observed with and without the addition of cells as shown in Figure 3c, indicating that body temperature might stimulate interactions between collagen molecules and cell surfaces. Moreover, when the conditions changed to body temperature and neutral pH, a significant decrease of triple-helical peaks was observed both with and without added cells. Additionally, the disappearance of triple-helical peaks under these conditions proceeded fastest—12 h compared with 20 h at both pH 7 and 25 °C (Figure 3b), as well as pH 4 and 37 °C (Figure 3c). The supernatants of these collagen solutions with 1×10^4 cells under different conditions were also examined. As shown in Supplementary Figure S4, no triple-helical peaks of collagen molecules were observed at pH 7, whereas the pH 4 samples showed weak triple-helical peaks. These findings may be because low pH conditions hindered the interactions between collagen molecules and cell surfaces.

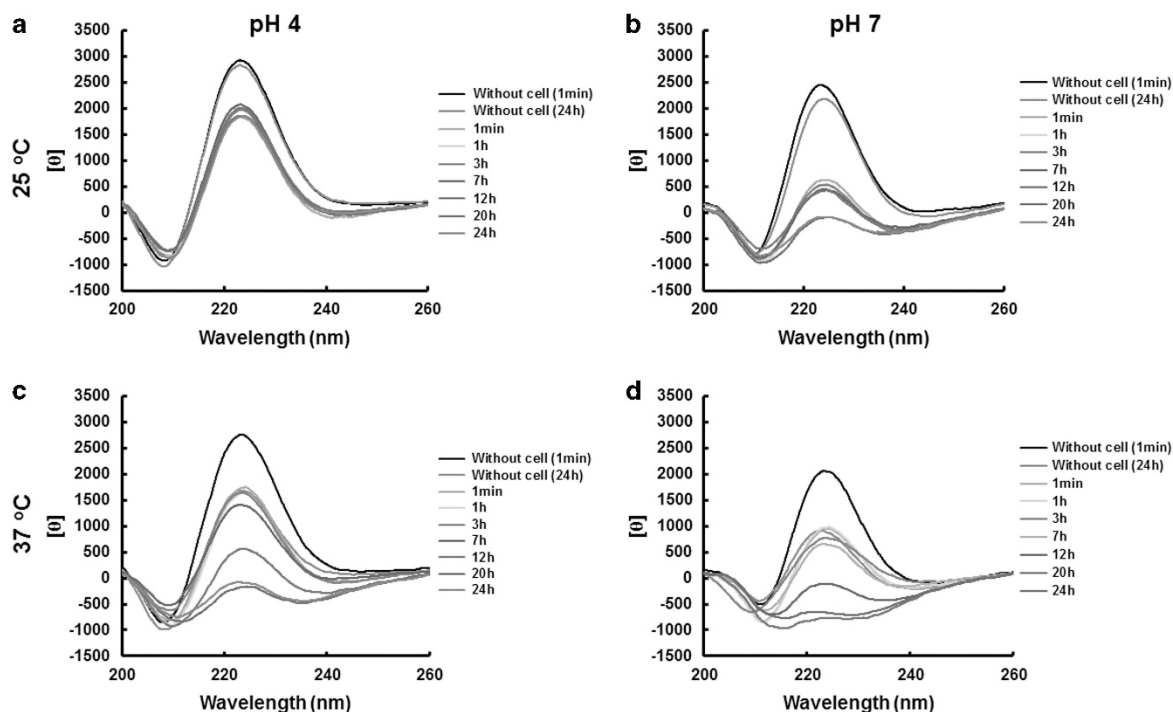


Figure 3 Variation of circular dichroism (CD) spectra of 0.003 wt% collagen solutions without or with 1×10^4 living cells in pH 4 or 7 solutions at (a, b) 25 °C or (c, d) 37 °C during a 24-h incubation. A full color version of this figure is available at *Polymer Journal* online.

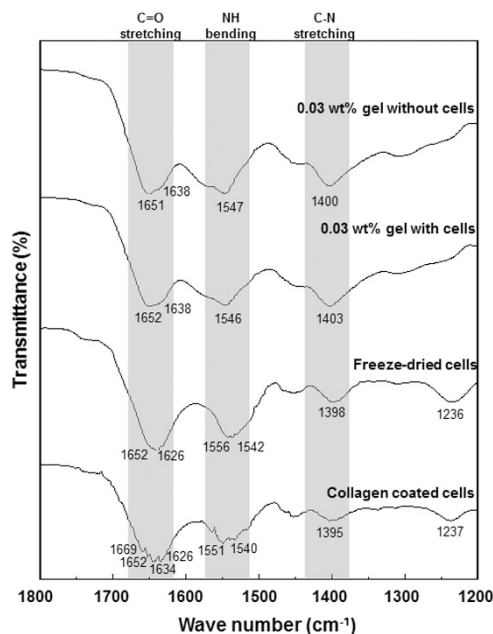


Figure 4 Fourier transform infrared (FTIR) spectra of 0.03 wt% collagen gels with and without cells as well as collagen-coated cells under room temperature. Approximately 1×10^6 cells were contained in the cell containing samples.

Collagen-coated cells were also used for CD spectral analysis. We previously reported high cell viability ($>95\%$) after coating procedures and showed good proliferation during a 4-day culture.²² As shown in Supplementary Figure S5, all samples at various temperatures and pH conditions showed no triple-helical peaks of collagen molecules, which may be because the balance of cells and collagen

molecules was quite different. Accordingly, no typical triple-helical peaks of collagen molecules were observed.

Cell effects on functional group variation of collagen molecules

To evaluate the effects of cells on the functional groups of collagen molecules, we performed FTIR spectral analyses. Some researchers have reported FTIR spectra of natural collagen matrices^{28,29} and collagen–chitosan composite materials.³⁰ The amide I band, which exhibits a high sensitivity to conformational changes, is a frequently used spectral region for IR spectroscopic analysis of protein secondary structure. This band of $\nu_{C=O}$ is centered in the range $1650\text{--}1660\text{ cm}^{-1}$. Additionally, as shown in Supplementary Figure S6, detailed peaks at $\sim 1550\text{--}1800\text{ cm}^{-1}$ are assigned to proteins of collagen: the peaks at 1652 cm^{-1} have been assigned to α -helix, 1626 cm^{-1} to β -sheets, 1634 cm^{-1} to triple helix and 1646 cm^{-1} to random coils.^{31,32} The amide II band is located at $\sim 1540\text{--}1550\text{ cm}^{-1}$, which represents the complex nature comprising both the N–H bending vibration (δ_{NH}),³³ whereas the stretching vibration of C–N groups of amide III (ν_{C-N}) was found at $\sim 1400\text{--}1410\text{ cm}^{-1}$.³⁴ In the cases of living cells and cells covered by collagen nanofibers, a band centered at 1236 cm^{-1} originates from asymmetric phosphate stretching vibrations, which can be attributed to phosphodiester groups of nucleic acid in DNA.³⁵ This specific band can be observed in the results from living cells and cells covered by collagen nanofibers, indicating the existence of living cells after the coating procedures.

We also found C=O stretching peaks ($\nu_{C=O}$) of amide I at 1651 cm^{-1} , N–H bending (δ_{NH}) of amide II at 1547 cm^{-1} , and C–N stretching (ν_{C-N}) of amide III at 1400 cm^{-1} in 0.03 wt% freeze-dried collagen gels without added cells (Figure 4). Although 1×10^6 cells were added to the gels (0.03 wt% collagen gels with cells), none of the amide bands shifted, suggesting that the cells had no effect on the functional groups of the collagen molecules. To understand amides in freeze-dried cells, FTIR spectra of the cells were also measured.

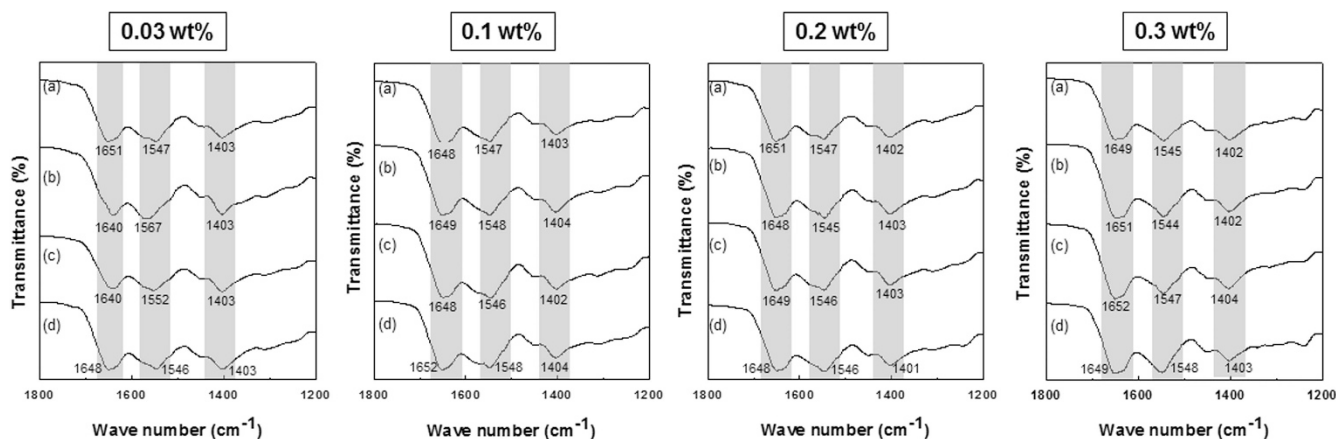


Figure 5 Fourier transform infrared (FTIR) spectra of collagen gels under different collagen concentrations (a) without cells and with (b) 1×10^4 , (c) 1×10^5 and (d) 1×10^6 cells.

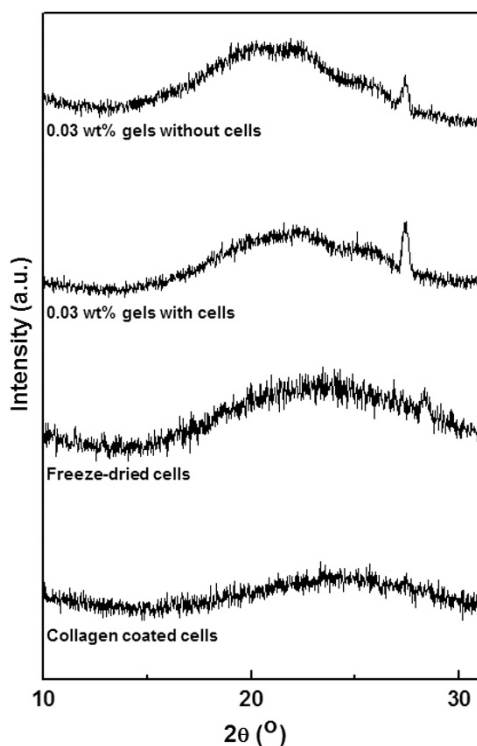


Figure 6 X-ray diffraction (XRD) diffractograms of 0.03 wt% collagen gels with and without cells and collagen-coated cells.

As shown in Figure 4, freeze-dried cells showed two peaks both for amide I ($\nu_{C=O}$), at 1652 and 1626 cm^{-1} , which may come from albumin and amyloid in the cells,³⁶ which are similar to the reported data of Choi *et al.*,³² who assigned peaks at 1650 and 1623 cm^{-1} to α -helices and β -sheet structures, respectively.³² Peaks at 1556 and 1542 cm^{-1} of amide II (δ_{NH}) were also observed in the freeze-dried cells.

In the case of 0.03 wt% collagen gels with and without the addition of 1×10^6 cells, peaks at 1652 and 1638 cm^{-1} , which represent α -helix and triple helix structures, respectively, were observed, indicating collagen fiber formation occurred during the incubation. In the case of 0.03 wt% collagen gels with 1×10^6 cells added, only α -helix and triple helix peaks were found, and specific peaks at 1626 and 1236 cm^{-1}

were not observed, possibly because of the balance in the amount of proteins of collagen molecules and cells. In the sample preparation, 0.4 mg of collagen and 2.7×10^{-2} mg of cells were used, making collagen 15 times more abundant. Owing to this huge disparity, the β -sheet peak at amide I might not be observed. Amide II peaks of gels containing cells had the same tendency as amide I bands. Freeze-dried cells showed two peaks at amide II for the same reason.

In the case of collagen-coated cells, we observed several peaks in amide I bands: α -helix (1652 cm^{-1}), β -sheet (1626 cm^{-1}), triple helix (1634 cm^{-1}) and β -turn (1669 cm^{-1}),^{37,38} belonging to both collagen molecules and cells. As with freeze-dried cells, two peaks at amide II bands were also observed. If the addition of cells in the collagen gels affects the amide bands by, for example, changing the conditions for hydrogen bonding with water molecules, peak shifts for the α -helices should be observed. However, no peak shift was found in samples containing cells, suggesting that there was no significant effect of the cells on collagen amide bands. The C–N stretching peak of amide III at 1400 cm^{-1} showed no peak shift because C–N stretching is not affected by changes in the surrounding environment, such as in hydrogen bonding. Amide I and amide II bands are usually influenced by changing conditions in hydrogen bonding, such as α -helices and β -sheets, but C–N stretching is usually independent of this effect. This may be the reason collagen gels and cells showed the same peak.

To understand the relationship between collagen concentration and cell number, amide bands of all samples were compared. As shown in Figure 5, α -helix and triple helix peaks at amide I show no difference regardless of the collagen concentration or cell number. Additionally, amide I and amide II bands revealed no shift under any conditions owing to the same reason. The amount of cells was much lower than the amount of collagen in all samples.

From the results of the FTIR analysis, we found that no cell effect was observed on functional groups and amide bands of collagen molecules on 3D cell cultures of type I collagen matrices.

Cell effect on molecular orientation of collagen molecules

To understand the effect of cells on the molecular orientation of collagen molecules, XRD analysis was performed. Different from the XRD diffraction of pure collagen fibers, where $2\theta = 7^\circ$, 20° and 31° ,³⁹ 0.03 wt% collagen gels with or without cells showed almost the same broad peak at $2\theta = 23^\circ$, which is the diffraction pattern of typical collagen gels as shown in Figure 6.^{40–42} This may be due to interactions of collagen molecules and inorganic salts or organic

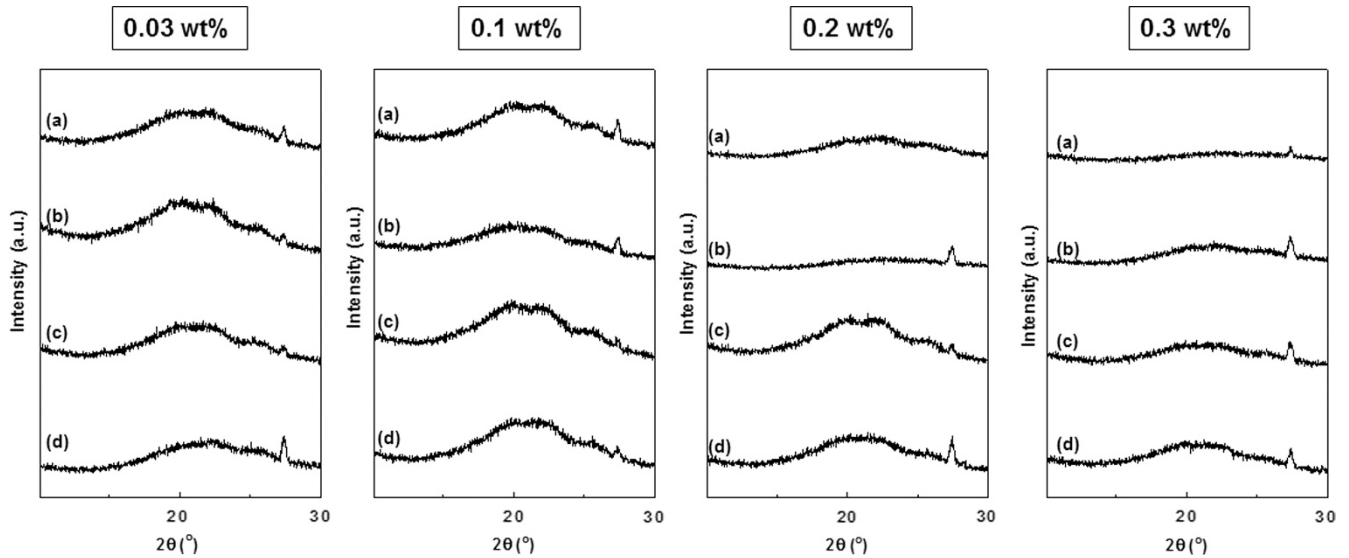


Figure 7 X-ray diffraction (XRD) diffractograms of collagen gels under different concentrations (a) without cells and with (b) 1×10^4 , (c) 1×10^5 , and (d) 1×10^6 cells.

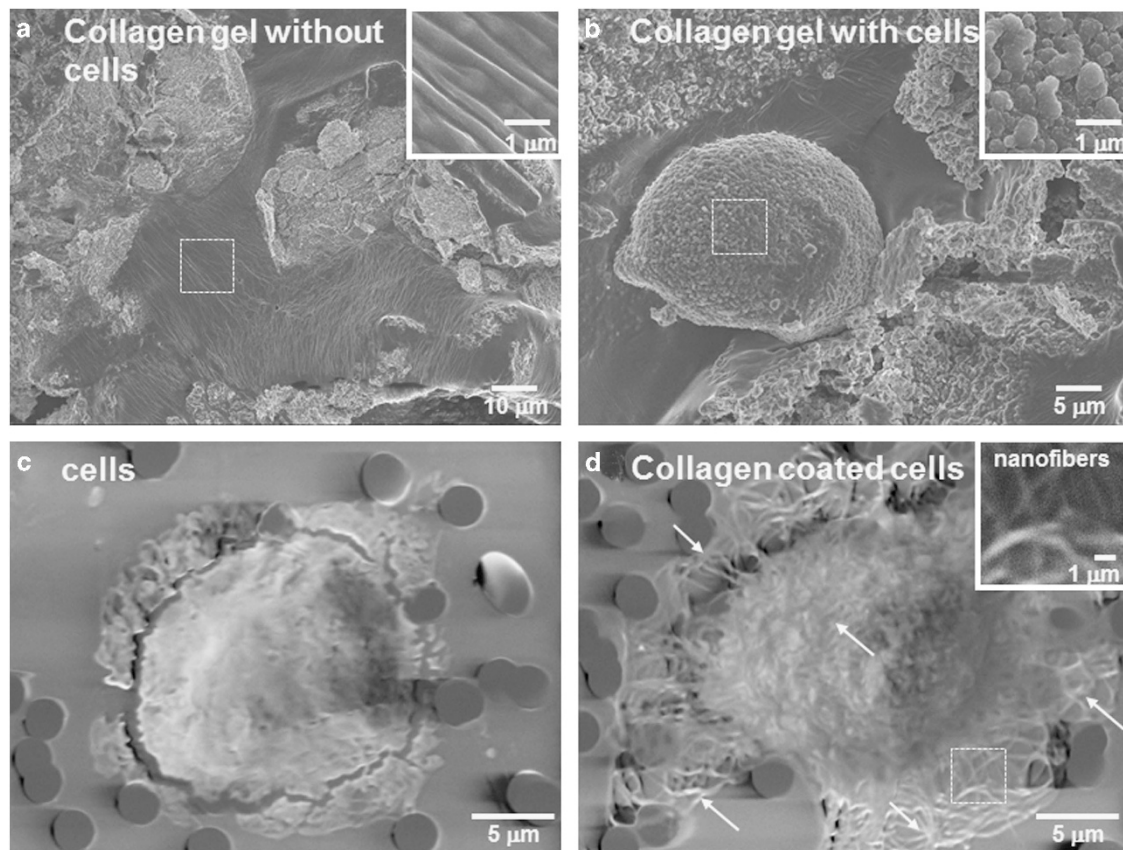


Figure 8 Scanning electronic microscope (SEM) images of (a) 0.03 wt% collagen gels without cells, (b) 0.03 wt% collagen gels with cells after 24 h of incubation, (c) cells and (d) collagen-coated cells after a 20 min coating procedure (arrows represent collagen nanofibers).

compounds inside the culture medium. Additionally, as mentioned in the previous description, there was a huge imbalance in the amounts of collagen molecules and cells, resulting in little impact of cells versus the collagen gels. In the case of freeze-dried cells, the results showed a broad peak from $2\theta = 20^\circ - 30^\circ$, identical to the peaks for freeze-dried

collagen-coated cells. The strong peak at $2\theta = 27^\circ$ was assigned to inorganic salts, CaCl_2 and NaCl , in the culture medium.^{43,44} From these results, we conclude that the added cells did not show any effect on the orientation of collagen fibers in the hydrogel or on the cell surfaces.

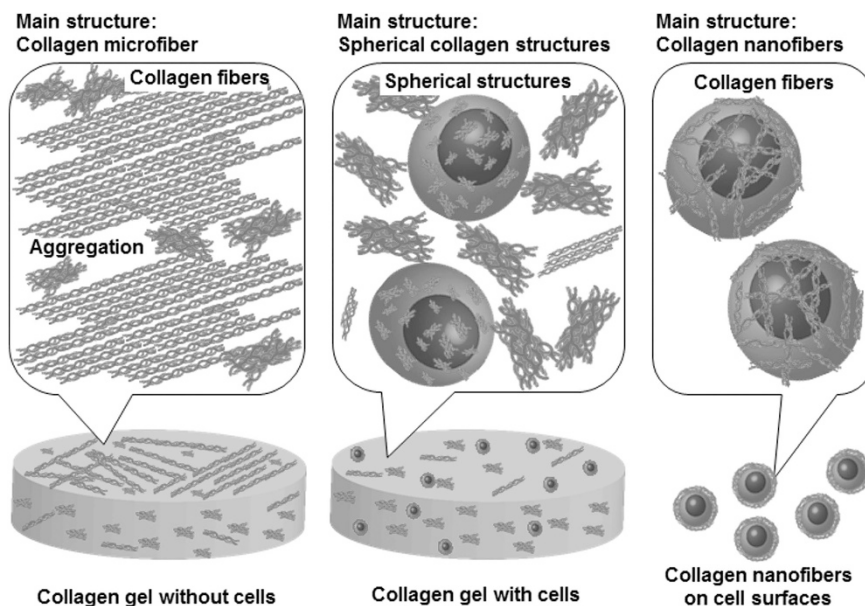


Figure 9 Schematic illustration of estimated structures of collagen molecules. Microfibers and spherical structures are the main collagen structures in collagen gel without or with cells, respectively. Nanofibers are main structures in collagen-coated cells. A full color version of this figure is available at *Polymer Journal* online.

To understand the relationship between collagen concentration and cell number, the XRD analyses of all samples prepared in this study were compared. As shown in Figure 7, a broad peak at $2\theta = 23^\circ$ was considered a typical collagen fiber, and $2\theta = 20^\circ\text{--}30^\circ$ was found when cells were added, suggesting that the addition of cells did not affect the molecular orientation of collagen molecules regardless of collagen concentration and cell number.

Cell effect on morphological changes to collagen gels

Finally, we observed the effect of adding cells on macroscopic collagen fiber formations using SEM observations. The freeze-dried 0.03 wt% collagen gels are shown in Figure 8a. The surface of the hydrogel partially showed aligned fiber morphology with fibers $\sim 0.3\ \mu\text{m}$ in diameter. However, 10–100 μm aggregates composed of spherical structures with submicrometer diameters were observed through cracks under the gel surface. Ulrich *et al.*⁴⁵ reported on 3D cultures of glioblastoma multiforme cells in collagen-based hydrogels and SEM observations of these gels. They also reported on the assembly of 0.2- μm -sized collagen fibers and disordered aggregation.⁴⁵ When 1×10^6 cells were added to collagen gels, fiber structures were not prominently observed (Figure 8b). Interestingly, submicrometer spherical collagens were adsorbed on cell surfaces homogeneously, and cells attached onto collagen aggregates. When we observed collagen gels with higher concentrations (0.1–0.3 wt%), it was difficult to find cells, perhaps due to the disproportionate amount of collagen compared with the amount of cells (Supplementary Figure S7). From these results, we found that cells cultured in collagen hydrogels affected the morphology of collagen fibers. These results suggested the possibility of cellular mechanotransduction in the structural rearrangement of collagen fibers in collagen gels.

To observe cell surfaces under wet conditions, we used a low-voltage SEM instrument (LVSEM, Miniscope TM3030; Hitachi). This instrument does not require osmium coating, alcoholic dehydration and freezing (needing only formalin fixation and TI blue staining). However, the resolution of this instrument is lower than that of field

emission-SEM. Using this instrument, realistic soft and wet conditions on the surface of the cellular microenvironment can be observed. We carefully observed cell surfaces with and without collagen nanofiber coatings. High-density meshwork structures were observed on surfaces with collagen nanofiber coatings in Figure 8d, whereas there were no fiber structures on uncoated cell surfaces in Figure 8c. Approximately 200 nm collagen fibers were coated on the cell surfaces, and some fibers were spread out on the cell surfaces. Collagen fiber meshwork structures found in this experiment seem to be similar to natural ECM fiber matrices in the body.

CONCLUSION

In summary, the effects of cells on collagen properties, functional groups and molecular orientation of collagen molecules were characterized via CD, FTIR and XRD spectral analyses as well as SEM observations. From the CD spectral results, we know that temperature, pH and the presence of cells had a great impact on the collagen molecules. Body temperature, neutral conditions and the addition of cells affected triple helix peaks due to aggregations of collagen molecules. The results of both FTIR and XRD spectra showed no effect of the cells on functional group amide I bands or on the molecular orientation of the collagen molecules, suggesting that the addition of cells inside the 3D collagen gels did not harm the collagen molecules. In the end, as shown in Figure 9, we observed that collagen gels presented fiber structures and submicrometer aggregation of collagen on gel surfaces. Cellular mechanotransduction based on morphology, thickness and nanostructures of the collagen matrix may be expected. In the case of collagen-coated cells, nanometer-sized collagen fibers were found on cell surfaces with some fibers spread out around the cells. From these results, we proved that cells do not affect the properties of collagen molecules, although macroscopic morphological aggregation occurred in collagen gels as well as coating on cell surfaces. This is the first study that describes the effect of cells on collagen molecules, which are widely used in 3D culture models and in the fabrication of 3D tissues.

ACKNOWLEDGEMENTS

This work was supported by the NEXT Program (LR026), a Grant-in-Aid for Scientific Research (S) and the SENTAN-JST Program. We also thank Mrs Kimura for her technical assistance.

- 1 Calderwood, D. A., Tuckwell, D. S., Eble, J., Kühn, K. & Humphries, M. J. The integrin $\alpha 1$ a-domain is a ligand binding site for collagens and laminin. *J. Biol. Chem.* **272**, 12311–12317 (1997).
- 2 Jiang, F., Hörber, H., Howard, J. & Müller, D. J. Assembly of collagen into microribbons: effects of pH and electrolytes. *J. Struct. Biol.* **148**, 268–278 (2004).
- 3 Harris, A. K., Wild, P. & Stopak, D. Silicone rubber substrata: a new wrinkle in the study of cell locomotion. *Science* **208**, 177–179 (1980).
- 4 Leikina, E., Merts, M. V., Kuznetsova, N. & Leikin, S. Type I collagen is thermally unstable at body temperature. *Proc. Natl Acad. Sci. USA* **99**, 1314–1318 (2002).
- 5 Harris, J. R. & Reiber, A. Influence of saline and pH on collagen type I fibrillogenesis *in vitro*: fibril polymorphism and colloidal gold labelling. *Micron* **38**, 513–521 (2007).
- 6 Abbott, A. Cell culture: biology's new dimension. *Nature* **424**, 870–872 (2003).
- 7 Loessner, D., Stok, K. S., Lutolf, M. P., Hutmacher, D. W., Clements, J. A. & Rizzi, S. C. Bioengineered 3D platform to explore cell-ECM interactions and drug resistance of epithelial ovarian cancer cells. *Biomaterials* **31**, 8494–8506 (2010).
- 8 Sung, K. E., Su, G., Pehlke, G., Trier, S. M., Eliceiri, K. W., Kelly, P. J., Friedl, A. & Beebe, D. J. Control of 3-dimensional collagen matrix polymerization for reproducible human mammary fibroblast cell culture in microfluidic devices. *Biomaterials* **30**, 4833–4841 (2009).
- 9 Chevallay, B. & Herbage, D. Collagen-based biomaterials as 3D scaffolds for cell cultures: applications for tissue engineering and gene therapy. *Med. Biol. Eng. Comput.* **38**, 211–218 (2000).
- 10 Thernistocleous, G. S., Katopodis, H., Sourla, A., Lembessis, P., Doillon, C. J., Soucacos, P. M. & Koutsilieris, M. Three-dimensional type I collagen cell culture systems for the study of bone pathophysiology. *In Vivo* **18**, 687–696 (2004).
- 11 Viney, M. E., Bullock, A. J., Day, M. J. & MacNeil, S. Co-culture of intestinal epithelial and stromal cells in 3D collagen-based environments. *Regen. Med.* **4**, 397–406 (2009).
- 12 Ko, Y. G., Kawazoe, N., Tateishi, T. & Chen, G. Preparation of novel collagen sponges using an ice particulate template. *J. Bioact. Compat. Poly.* **25**, 360–373 (2010).
- 13 Beier, J. P., Klumpp, D., Rudisile, M., Dersch, R., Wendorff, J. H., Bleiziffer, O., Arkudas, A., Polykandriotis, E., Horch, R. E. & Kneser, U. Collagen matrices from sponge to nano: new perspective for tissue engineering of skeletal muscle. *BMC Biotechnol.* **9**, 34 (2009).
- 14 Chaubaroux, C., Vrana, E., Debry, C., Schaaf, P., Senger, B., Voegel, J. C., Haikel, Y., Ringwald, C., Hemmerlé, J., Lavalle, P. & Boulmedais, F. Collagen-based fibrillar multilayer films cross-linked by a natural agent. *Biomacromolecules* **13**, 2128–2135 (2012).
- 15 Kim, T. K., Park, S. H., Chung, H. J., Yang, D. Y. & Park, T. G. Microstructured scaffold coated with hydroxyapatite/collagen nanocomposite multilayer for enhanced osteogenic induction of human mesenchymal stem cells. *J. Mater. Chem.* **20**, 8927–8933 (2010).
- 16 Janin-Manificat, H., Rovère, M. R., Galiacy, S. D., Malecaze, F., Hulmes, D. J. S., Moali, C. & Damour, O. Development of *ex vivo* organ culture models to mimic human corneal scarring. *Mol. Vis.* **18**, 2896–2908 (2012).
- 17 Kim, H. S., Lim, J. B., Min, Y. H., Lee, S. T., Lyu, C. J., Kim, E. S. & Kim, H. O. *Ex vivo* expansion of human umbilical cord blood CD34⁺ cells in a collagen bead-containing 3-dimensional culture system. *Int. J. Hematol.* **78**, 126–132 (2003).
- 18 Jokinen, J., Dadu, E., Nykvist, P., Käpylä, J., White, D. J., Ivaska, J., Vehviläinen, P., Reunanen, H., Larjava, H., Häkkinen, L. & Heino, J. Integrin-mediated cell adhesion to type I collagen fibrils. *J. Biol. Chem.* **279**, 31956–31963 (2004).
- 19 Kirchofer, D., Languino, L. R., Ruoslahti, E. & Pierschbacher, M. D. Alpha 2 beta 1 integrins from different cell types show different binding specificities. *J. Biol. Chem.* **265**, 615–618 (1990).
- 20 Giancotti, F. G. & Ruoslahti, E. Integrin signaling. *Science* **285**, 1028–1032 (1999).
- 21 Lutolf, M. P. & Hubbell, J. A. Synthetic biomaterials as instructive extracellular microenvironments for morphogenesis in tissue engineering. *Nat. Biotechnol.* **23**, 47–55 (2005).
- 22 Liu, C. Y., Matsusaki, M. & Akashi, M. The construction of cell-density controlled three-dimensional tissues by coating micrometer-sized collagen fiber matrices on single cell surfaces. *RSC Adv.* **4**, 46141–46144 (2014).
- 23 Fujioka, K., Maeda, M., Hojo, T. & Sano, A. Protein release from collagen matrices. *Adv. Drug Deliv. Rev.* **31**, 247–266 (1998).
- 24 Hongo, C., Matsusaki, M., Nishida, K. & Akashi, M. Development of a collagen hydrogel with high mechanical strength by a simple orientation method for triple-helix. *Chem. Lett.* **37**, 1254–1255 (2008).
- 25 Shan, A., Brugnano, J., Sun, S., Vase, A. & Orwin, E. The development of a tissue-engineered cornea: biomaterials and culture methods. *Pediatr. Res.* **63**, 535–544 (2008).
- 26 Brown, E. M., Farrell, H. M. Jr. & Wildermuth, R. J. Influence of natural salts on the hydrothermal stability of acid-soluble collagen. *J. Protein Chem.* **19**, 85–92 (2000).
- 27 Calderwood, D. A., Tuckwell, D. S., Eable, J., Kühn, K. & Humphries, M. J. The integrin $\alpha 1$ A-domain is a ligand binding site for collagens and laminin. *J. Biol. Chem.* **272**, 12311–12317 (1997).
- 28 Campos Vidal, B. & Mello, M. L. S. Collagen type I amide I band infrared spectroscopy. *Micron* **42**, 283–289 (2011).
- 29 Dong, A., Huang, P. & Caughey, W. S. Protein secondary structures in water from second-derivative amide I infrared spectra. *Biochem* **29**, 3303–3308 (1990).
- 30 Fernandes, L. L., Resende, C. X., Tavares, D. S. & Soares, G. A. Cytocompatibility of chitosan and collagen-chitosan scaffolds for tissue engineering. *Polímeros* **21**, 1–6 (2011).
- 31 Lai, J. Y., Lue, S. J., Cheng, H. Y. & Ma, D. H. Effect of matrix nanostructure on the functionality of carboxyamide cross-linked amniotic membranes as limbal epithelial cell scaffolds. *J. Biomed. Nanotechnol.* **9**, 2048–2062 (2013).
- 32 Choi, B. G., Park, M. H., Cho, S. H., Joo, M. K., Oh, H. J., Kim, E. H., Park, K., Han, D. K. & Jeong, B. *In situ* thermal gelling polypeptide for chondrocytes 3D culture. *Biomaterials* **31**, 9266–9272 (2010).
- 33 Vileno, B., Heney, S., Sienkiewicz, A., Marcoux, P. R., Miller, L. M. & Forró, L. Evidence of lipid peroxidation and protein phosphorylation in cells upon oxidative stress photo-generated by fullerenes. *Biophys. Chem.* **152**, 164–169 (2010).
- 34 Baia, L., Baia, M., Danciu, V., Albu, M. G., Coşoveanu, V., Ordăchescu, D. & Trandafir, V. Type I collagen-TiO₂ aerogel based biocomposites. *J. Optoelectron Adv. Mater.* **10**, 933–936 (2008).
- 35 Bonda, M., Perrin, V., Vileno, B., Runne, H., Kretlow, A., Forró, L., Luthi-Carter, R., Miller, L. M. & Jeney, S. Synchrotron infrared microspectroscopy detecting the evolution of huntington's disease neuropathology and suggesting unique correlates of dysfunction in white versus gray brain matter. *Anal. Chem.* **83**, 7712–7720 (2011).
- 36 Cheng, P. N., Liu, C., Zhao, M., Eisenberg, D. & Nowick, J. S. Amyloid β -sheet mimics that antagonize protein aggregation and reduce amyloid toxicity. *Nat. Chem.* **4**, 927–933 (2012).
- 37 Petitbois, C., Gouspillou, G., Wehbe, K., Delage, J. P. & Déleris, G. Analysis of type I and IV collagens by FT-IR spectroscopy and imaging for a molecular investigation of skeletal muscle connective tissue. *Anal. Bioanal. Chem.* **386**, 1961–1966 (2006).
- 38 Belbachir, K., Noreen, R., Gouspillou, G. & Petitbois, C. Collagen types analysis and differentiation by FTIR spectroscopy. *Anal. Bioanal. Chem.* **395**, 829–837 (2009).
- 39 Thanikaivelan, P., Narayanan, N. T., Pradhan, B. K. & Ajayan, P. M. Collagen based magnetic nanocomposites for oil removal applications. *Sci. Rep.* **2**, 230 (2012).
- 40 Mohd Nasir, N. F., Raha, M. G., Kadri, N. A., Sahidan, S. I., Rampado, M. & Azlan, C. A. The study of morphological structure, phase structure and molecular structure of collagen-PEO 600K blends for tissue engineering application. *Am. J. Biochem. Biotechnol.* **2**, 175–179 (2006).
- 41 Saska, S., Teixeira, L. N., Oliveira, P. T., Gaspar, A. M. M., Ribeiro, S. J. L., Messaddeq, Y. & Marchetto, R. Bacterial cellulose-collagen nanocomposite for bone tissue engineering. *J. Mater. Chem.* **22**, 22102–22112 (2012).
- 42 Xia, Z., Villa, M. M. & Wei, M. A biomimetic collagen-apatite scaffold with a multi-level lamellar structure for bone tissue engineering. *J. Mater. Chem. B* **2**, 1998–2007 (2014).
- 43 Lu, J., Luo, M., Lei, H. & Li, C. Epoxidation of propylene on NaCl-modified silver catalysts with air as the oxidant. *Appl. Catal. A* **237**, 11–19 (2002).
- 44 Sugino, A., Miyazaki, T. & Ohtsuki, C. Apatite-forming ability of polyglutamic acid hydrogels in a body-simulating environment. *J. Mater. Sci.* **19**, 2269–2274 (2008).
- 45 Ulrich, T. A., Jain, A., Tanner, K., MacKay, J. L. & Kumar, S. Probing cellular mechanobiology in three-dimensional culture with collagen-agarose matrices. *Biomaterials* **31**, 1875–1884 (2010).

Supplementary Information accompanies the paper on Polymer Journal website (<http://www.nature.com/pj>)